The findings presented here have important implications for estimates of aerosol effects on climate forcing. Aerosols can either invigorate clouds, increasing cloud fraction and height (a result of the microphysical effects), or inhibit clouds, decreasing cloud fraction and height (a result of aerosol absorption). These two processes are superimposed, and affect clouds of varying vertical development differently. Small shallow clouds will be mostly inhibited throughout the range of τ, leading to net positive climate forcing (warming), whereas medium- and high-level clouds will be strongly invigorated in the low-τ range, leading to negative climate forcing (cooling) and the inhibition of higher aerosol loading, which again leads to warming.

Initial cloud fraction plays a critically important role in determining the balance between the two effects. Cloud fields with large cloud coverage will be affected mostly by microphysics (invigoration), whereas fields with low fraction will be inhibited strongly by aerosol absorption. This can further polarize the atmospheric regimes in such a way that the overcast mode will last longer with thicker clouds, whereas scattered cloud fields will be suppressed, resulting in smaller coverage of thinner clouds. Such redistribution of energy not only changes the climate radiative energy balance but also can change local and regional dynamics and precipitation patterns.

These results should help provide a better understanding of the processes involved in making estimates of climate forcing through cloud/aerosol interaction. Furthermore, these results will be useful in their current form for incorporation in or testing of cloud-resolving or climate models.

References and Notes

1. Y. J. Kaufman, I. Koren, *Science* **313**, 655 (2006).
2. H.-F. Graf, *Science* **203**, 1309 (2004).
3. S. Twomey, *J. Atmos. Sci.* **34**, 1149 (1977).
4. H. Jiang, G. Feingold, *J. Geophys. Res.* **111**, D01202 (2006).
5. D. Rosenfeld, *Science* **287**, 1793 (2000).
6. I. Koren, Y. J. Kaufman, L. A. Remer, J. V. Martins, *Science* **303**, 1342 (2004).
7. G. Feingold, H. Jiang, J. Y. Harrington, *Geophys. Res. Lett.* **32**, L02804 (2005).
8. G. Feingold, L. A. Remer, J. Ramaprasad, Y. J. Kaufman, *J. Geophys. Res.* **106**, 22907 (2001).
9. Y. J. Kaufman, I. Koren, L. A. Remer, D. Rosenfeld, Y. Rudich, *Proc. Natl. Acad. Sci. U.S.A.* **102**, 11207 (2005).
10. I. Koren, Y. J. Kaufman, L. A. Remer, D. Rosenfeld, Y. Rudich, *Geophys. Res. Lett.* **32**, 10.1029/2005GL023187 (2005).
11. See supporting data on *Science* Online.
12. A. S. Ackerman *et al.*, *Science* **288**, 1042 (2000).
13. Y. J. Kaufman, T. Nakajima, *J. Appl. Meteorol.* **32**, 729 (1993).
14. M. Wetzel, L. Stowe, *J. Geophys. Res.* **104**, 31287 (1999).
15. A. Khain, D. Rosenfeld, A. Pokrovsky, *Q. J. R. Meteorol. Soc.* **131**, 2639 (2005).
16. G. Myhre *et al.*, *Atmos. Chem. Phys.* **7**, 3081 (2007).
17. S. Platnick *et al.*, *IEEE Trans. Geosci. Remote Sens.* **41**, 459 (2003).
18. R. C. Levy, L. Remer, S. Mattoo, E. Vermote, Y. J. Kaufman, *J. Geophys. Res.* **112**, D13211 (2007).
19. M. D. King *et al.*, *IEEE Trans. Geosci. Rem. Sens.* **41**, 442 (2003).
20. C. A. Nobre, L. F. Mattos, C. P. Dereczynski, T. A. Tarasova, I. V. Trosnikov, *J. Geophys. Res.* **103**, 31809 (1998).
21. J. I. Brennan, Y. J. Kaufman, I. Koren, R.-R. Li, *IEEE Trans. Geosci. Remote Sens.* **43**, 911 (2005).
22. I. Koren, L. Remer, K. Longo, *Geophys. Res. Lett.* **34**, L20404 10.1029/2007GL031530 (2007).
23. M. O. Andreae *et al.*, *Science* **303**, 1337 (2004).
24. I. Koren, L. A. Remer, Y. J. Kaufman, Y. Rudich, J. V. Martins, *Geophys. Res. Lett.* **34**, L08805 (2007).
25. R. J. Charlson, A. S. Ackerman, F. A. Bender, T. L. Anderson, Z. Liu, *Tellus B Chem. Phys. Meterol.* **59**, 715 (2007).

26. This paper is dedicated to the memory of Yoram J. Kaufman, a dear friend and a brilliant scientist. This research was supported in part by the Israel Science Foundation (grant no. 1355/06), and NASA's Interdisciplinary Science Program under the direction of H. Maring. I.K. is the incumbent of the Benjamin H. Swig and Jack D. Weiler career development chair at the Weizmann Institute.

Supporting Online Material

www.sciencemag.org/cgi/content/full/321/5891/946/DC1
SOM Text
Figs. S1 to S5
References

16 April 2008; accepted 8 July 2008
10.1126/science.1159185

Ferruginous Conditions Dominated Later Neoproterozoic Deep-Water Chemistry

Donald E. Canfield,[1]* Simon W. Poulton,[2] Andrew H. Knoll,[3] Guy M. Narbonne,[4] Gerry Ross,[5] Tatiana Goldberg,[2] Harald Strauss[6]

Earth's surface chemical environment has evolved from an early anoxic condition to the oxic state we have today. Transitional between an earlier Proterozoic world with widespread deep-water anoxia and a Phanerozoic world with large oxygen-utilizing animals, the Neoproterozoic Era [1000 to 542 million years ago (Ma)] plays a key role in this history. The details of Neoproterozoic Earth surface oxygenation, however, remain unclear. We report that through much of the later Neoproterozoic (<742 ± 6 Ma), anoxia remained widespread beneath the mixed layer of the oceans; deeper water masses were sometimes sulfidic but were mainly Fe^{2+}-enriched. These ferruginous conditions marked a return to ocean chemistry not seen for more than one billion years of Earth history.

Early in Earth history, the deep oceans contained dissolved ferrous Fe, as documented by the widespread deposition of banded Fe formations (*1*). This condition expressed low atmospheric oxygen and low seawater sulfate concentrations in combination (*2*). The former limited the transport of oxygen into the deep ocean, whereas the latter limited rates of sulfide production by sulfate-reducing prokaryotes; without the low sulfate, the oceans would have been sulfidic, something like the modern Black Sea. Indeed, current models suggest that sulfidic deep-ocean conditions did become widespread around 1840 million years ago (Ma) as a result of increasing sulfate concentrations, and that this condition may have persisted through much of the Mesoproterozoic Era [1.6 to 1.0 billion years ago (Ga)] [(*3*–*6*); however, see (*7*) for another view].

The emergence of diverse animals by the end of the Neoproterozoic Era indicates a probable change to more oxic ocean and atmospheric conditions (*8*), but the course of this change is unclear. For example, despite a long-term increase in seawater oxygenation, iron formations recurred in association with globally extensive Neoproterozoic glaciations (*9*). An important pillar of the Snowball Earth hypothesis that maintains the Earth was completely covered in ice during significant periods of the Neoproterozoic, these iron formations are thought to represent the accumulation of Fe^{2+} in an ice-capped anoxic ocean (*10*, *11*). Ferruginous deep-ocean waters were also associated with the later Gaskiers ice age (580 Ma) (*12*), but deep-water oxygenation followed deglaciation, at least on the Avalon Peninsula, Newfoundland. Was this deep-water oxygenation, however, local or global, and was it the first time that oxygen pervaded deep waters during the Neoproterozoic era? Also, what is the relationship between short, ice age–associated intervals of iron deposition and the broader evolution of Neoproterozoic atmospheric and oceanic chemistry? Finally, and more broadly, how does Neoproterozoic ocean chemistry link the probable widespread occurrence of Mesoproterozoic sulfidic marine conditions with the predominantly oxic conditions of the Phanerozoic Eon (the past 542 Ma)? These outstanding issues invite further exploration of Neoproterozoic ocean chemistry.

We evaluated the redox chemistry of the marine water column by considering the speciation of Fe in well-preserved Neoproterozoic sedimentary rocks. With a calibrated Fe extraction proce-

[1]Nordic Center for Earth Evolution and Institute of Biology, Campusvej 55, University of Southern Denmark, 5230 Odense, Denmark. [2]School of Civil Engineering and Geosciences, Newcastle University, Drummond Building, Newcastle upon Tyne NE1 7RU, UK. [3]Botanical Museum, Harvard University, Cambridge, MA 02138, USA. [4]Department of Geological Sciences and Geological Engineering, Queen's University, Kingston, Ontario K7L 3N6, Canada. [5]Kupa'a Farm, Post Office Box 458, Kula, HI 96790, USA. [6]Geologisch-Paläontologisches Institute der Universität Münster, Corrensstrasse 24, Münster 48149, Germany.

*To whom correspondence should be addressed. E-mail: dec@biology.sdu.dk

dure (*13*), we separated Fe into forms that are biogeochemically highly reactive and those that are not. In modern marine sediments depositing under an oxic water column, highly reactive Fe (FeHR) constitutes a maximum of 38% of the total Fe pool (*14*). In contrast, sediments accumulating under an anoxic water column can have a much higher proportion of FeHR (*15*). Thus, when the ratio of FeHR to total Fe (FeHR/FeT) is greater than 0.38, deposition from an anoxic water body is indicated. In many instances, our samples come from surface outcrops (table S1), where some degree of post-exposure oxidation is difficult to discount. Most probably, however, even moderate surface weathering will have little influence on our final conclusions (*16*). Therefore, we used the principles outlined above to guide our interpretation of ancient seawater chemistry.

Fe speciation was determined for more than 700 individual samples from 34 different geologic formations, ranging in age from about 850 Ma in the middle Neoproterozoic to about 530 Ma in the Early Cambrian. Formation names, ages, an indication of depositional environment, and other notes are presented in Table 1. A complete discussion of chronology and depositional environment is presented in (*15*) and highlighted below where necessary. Speciation results, presented as FeHR/FeT, are plotted against time in Fig. 1A. We separated samples by depositional environment. Samples designated as "shallow shelf" were all deposited above the mean storm wave base. Those designated "outer shelf, shallow basin" were deposited in adjacent but deeper settings, below the mean storm wave base; these include samples deposited on the outer shelf and samples from epicontinental seas and rift basins where their position relative to the mean storm wave base had been influenced by changes in eustatic sea level. Our slope and deep basin samples are deep in an oceanographic sense, and most were deposited in passive margin settings with apparent open access to the global ocean (*15*).

Reactive Fe enrichments are common throughout the later Neoproterozoic (Fig. 1A), indicating frequent bottom-water anoxia in sediments deposited below the mean storm wave base. Reactive Fe enrichments are much less prevalent in shallow-shelf sediments, as would be expected; some of these are demonstrably oxic, such as the Bitter Springs Formation and the Quartzite and Multicolor Series from East Greenland, both associated with abundantly preserved cyanobacteria and stromatolites (*17*, *18*). Occasional high proportions of FeHR in shallow sediments could represent episodic anoxia in restricted environments such as lagoons or the preferential deposition of terrestrial Fe oxides in near-shore environments (*19*).

In some instances, in particular the Twitya Formation, western Canada, and the Tillite Group, East Greenland, our extraction results show little evidence of bottom-water anoxia (these sites are marked with asterisks on Fig. 1), but total Fe contents are greatly enriched as compared with average shale [4.7 weight percent (wt %) (*20*)]. In the Twitya Formation, FeT = 8.1 ± 2.1 wt %; in the Tillite Group, FeT = 7.23 ± 2.1 wt %. These iron concentrations generate Fe/Al ratios of 0.89 ± 0.19 in the Twitya Formation and 1.08 ± 0.18 in the Tillite Group, which are much higher than typically measured from oxic depositional settings [0.4 to 0.6 (*21*)] and, indeed, are comparable to those found in euxinic Black Sea sediments (*21*). Therefore, Fe/Al ratios in the Twitya Formation and Tillite Group provide independent evidence of Fe enrichment, and are fully consistent with enhanced Fe deposition from an anoxic water column (*21*). In these cases, high proportions of secondary silicate minerals such as chlorite indicate conversion (and thus loss) of unsulfidized FeHR during metamorphism (*21*).

As noted previously (*12*), clear evidence for the development of oxic deeper waters (represented by persistent FeHR/FeT ratios of well below 0.38) is seen at 580 Ma in the transition from the Gaskiers glaciation to the overlying Drook Formation on the Avalon Peninsula, Newfoundland. We identified similarly low FeHR/FeT in deep-water sediments from the Ediacaran upper Kaza Group, Caribou Mountains, western Canada. These sediments postdate the Marinoan glaciation, represented locally by the Old Fort Point Formation in the middle Kaza (*22*). About 1 km of stratigraphy separates our Upper Kaza samples from Old Fort rocks, and nearly 3 km more lie between the upper Kaza and basal Cambrian strata (*22*). Correlation of upper Kaza and post-Gaskiers successions is therefore possible but not certain. Nonetheless, upper Kaza data add to a growing body of evidence for widespread oxygenation of the global deep ocean around 580 to 560 Ma (*4*, *23*–*25*). Even so, oxygenation was not universal; our speciation results indicate that

Table 1. Formations, locations, and ages of the sections from this study. GC, Grand Canyon, United States; SA, South Australia; CM, Caribou Mountains, Canada; MM, Mackenzie Mountains, western Canada; YP, Yangtze Platform, South China; AP, Avalon Peninsula, Newfoundland; AB, Amadeus Basin, Australia; EG, East Greenland; SP, Spitzbergen, Svalbard; SS, Stuart Shelf, South Australia; SB, Siberia; DB, deep basin; OS, outer shelf and shallow basin, all below mean storm wave base; SS, shallow shelf, above mean storm wave base.

Formation	Location	Setting	Age range (Ma)*	Sample type
Kwangunt, Walcott Member	GC	OS	750–760	Core
Tapley Hill	SA	OS	665–697	Core
Apilla Tillite	SA	OS	698–700	Core
Brighton Limestone	SA	OS	663–665	Core
Kaza Group, Old Fort Point	CM	DB	608	Outcrop
Upper Kaza	CM	DB	580–573	Outcrop
Isaac	CM	DB	560–573	Outcrop
Twitya	MM	DB	650-697	Outcrop
Sheepbed	MM	DB	570–630	Outcrop
Doushantuo-a	YP	DB	570–631	Outcrop
Liuchapo-a	YP	DB	543–551	Outcrop
Niutitang-a	YP	DB	530–542	Outcrop
Niutitang (Xiaosi Member)	YP	DB	524–530	Outcrop
Mall Bay	AP	DB	581–583	Outcrop
Gaskiers	AP	DB	580–581	Outcrop
Drook	AP	DB	573–580	Outcrop
Briscal	AP	DB	569–570	Outcrop
Mistaken Point	AP	DB	564–567	Outcrop
Trepassey	AP	DB	562–564	Outcrop
Fermeuse	AP	DB	561–562	Outcrop
Bitter Springs	AB	SS	805	Outcrop
Quartzite Series	EG	SS	788–798	Outcrop
Multicolor Series	EG	SS	770–774	Outcrop
Limestone-Dolomite Series	EG	SS	750–755	Outcrop
Elbobreen	SP	OS	625–765	Outcrop
Dracoisen	SP	OS	620	Outcrop
Tillite Group	EG	OS	640–660	Outcrop
Canyon Formation	EG	OS	600	Outcrop
Woomera	SS	SS	625	Core
Arcoona ABC	SS	SS	620	Core
Elyuah	SS	OS	610	Core
Grants Bluff	SS	OS	590	Core
Upper Staraya	SB	SS	545	Outcrop
Kessyusa	SB	SS	540	Outcrop
Koftelv	EG	SS	530	Outcrop

*Not all sequences are well dated, so in many cases, age assignments are based on correlations with other sections, and in a few cases on educated guesses. See (*16*) for a full discussion of chronology.

parts of the deep ocean remained anoxic, even after this event.

What was the chemical nature of these anoxic deep waters? We addressed this by exploring further the speciation of FeHR. In particular, we evaluated the proportion of FeHR bound as sulfide phases (FeP/FeHR). Evidence from the Black Sea and other sulfidic (euxinic) basins shows that the ratio of FeP/FeHR commonly exceeds 0.8 under sulfidic water column conditions (*14*). When FeP/FeHR is less than this and the water column is anoxic, ferruginous water column conditions are indicated (*6*). FeP/FeHR ratios from samples in which FeHR/FeT suggests anoxia (when FeHR/FeT > 0.38) are plotted in Fig. 1. Typically, FeP/FeHR values fall well below 0.8, indicating ferruginous rather than sulfidic water-column conditions (*16*). Fe carbonates typically account for >20% of the reactive Fe pool in these samples (*15*), which rules out euxinic conditions, even in cases in which all of any original pyrite (FeS_2) was completely oxidized during weathering (*16*).

There are, however, two instances where sulfidic water-column conditions are clearly indicated: in parts of the Chuar Group, Grand Canyon, United States (~750 Ma), and the earliest Cambrian Niutitang Formation, Yangtze Platform, China (fig. S1). The Chuar Group deposited in a rift basin (*26*), but tidal influence is evident in shallow-water sequences (*26*), indicating, along with isotopic geochemistry and microfossil assemblages (*27*), probable open access to the global ocean. Our samples come mainly from distal black shales of the upper Walcott Member, which represents the deepest water of the Chuar Basin (*26*). As we have no other basinal samples contemporaneous with the Chuar, it is unresolved whether these sulfidic conditions represent a regional phenomenon or possible continuation of the deep marine sulfidic waters established during the Mesoproterozoic (*3*–*6*). Our finding of sulfidic bottom-water conditions at the Proterozoic-Cambrian boundary on the Yangtze platform reinforces previous studies of this region (*28*, *29*) and studies from Iran (*30*) and Oman (*31*), suggesting that sulfidic deep waters were widespread during the terminal Neoproterozoic and earliest Cambrian. Our data also show that on the Yangtze Platform, the sulfidic waters followed a long period of anoxic ferruginous conditions, and anoxic ferruginous conditions also followed this sulfidic interval (Fig. 1 and fig. S1).

A summary of our evidence for the development of Neoproterozoic ocean chemistry is given in Fig. 2. We have demonstrated that anoxic ferruginous conditions were common below the mean storm wave base in the latter half of the Neoproterozoic Era and, regionally at least, into the early Cambrian. Ferruginous waters formed in outer-shelf environments and shallow continental basins, as well as in deep basinal settings. Therefore, anoxic ferruginous marine deep waters were a general feature of later Neoproterozoic oceans, and not simply associated with Neoproterozoic glaciation, as previously thought. The ferruginous Neoproterozoic deep waters represent a return to the chemistry of much earlier, >1.8 Ga oceans (*1*).

Our new results reinforce previous work showing mid-Ediacaran (580 to 560 Ma) oxygenation of the deep ocean but show that this oxygenation was not universal and that anoxic conditions were also present. The spatial structure of this chemical mosaic is, however, unknown. We also show that, not surprisingly, shallow waters were typically well-oxygenated throughout the later Neoproterozoic and that, perhaps more surprisingly, sulfidic anoxic deep water was rare. Our sample set is large; nonetheless, it still provides only a series of geochemical snapshots in space and time. It is possible that ferruginous deep water first developed before the Sturtian ice age, that sulfidic

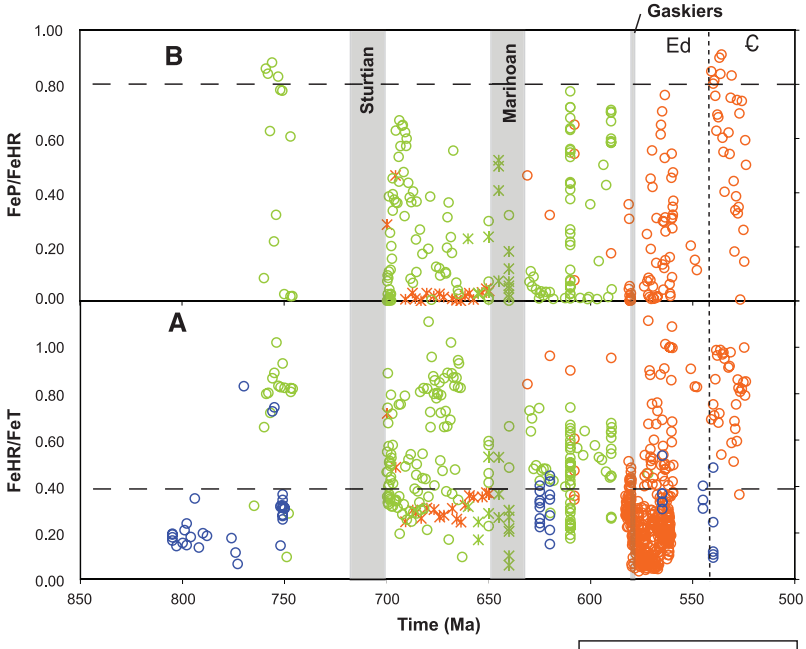

Fig. 1. Fe speciation as a function of time. (**A**) FeHR/FeT is shown. When the ratio exceeds 0.38, shown by the dashed line, this is evidence for deposition from an anoxic water column. As indicated in the key, samples are grouped into different depositional environments. Those samples designated with an asterisk have very high concentrations of total Fe and high ratios of total Fe to Al, which give independent evidence for anoxic deposition. These samples have probably lost FeHR during metamorphic conversion to unreactive Fe phases. The proportion of FeHR bound as FeS_2 is shown in (**B**). This proportion is given as FeP/FeHR. Only samples deposited below the mean storm wave base where anoxic deposition is indicated are plotted (FeHR/FeT ≥ 0.38). When this ratio exceeds 0.8, shown by the dashed line, deposition from a sulfidic water body is indicated, and ratios less than this are consistent with deposition from ferruginous waters. Only samples from the Chuar group and the Cambrian-Ediacaran boundary on the Yangtze Platform show evidence for sulfidic water column conditions [see SOM text for details and (*15*) for complete data]. The vertical dotted line indicates the Cambrian (Є)–Ediacaran (Ed) boundary.

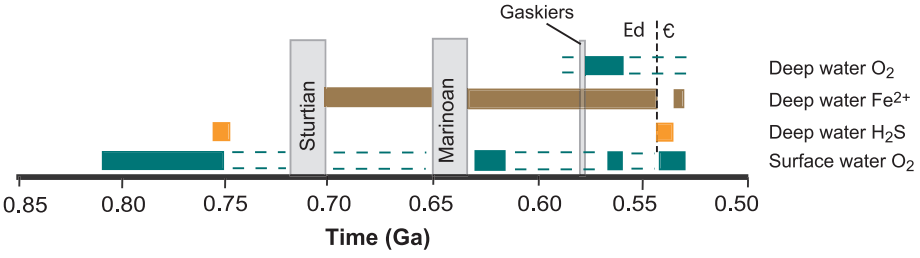

Fig. 2. A summary of our evidence of ocean-water chemical conditions through the last half of the Neoproterozoic and into the early Cambrian. Our results for deep-water chemistry do not necessarily reflect global trends but rather reflect the time course of our evidence for different deep-water chemical conditions. Deep water here means sediments deposited below the mean storm wave base. We extend evidence for deep-water oxygenation with dashed lines into pre-Gaskiers time, reflecting uncertainty in the age of the Upper Kaza Group, which shows evidence for oxic deep water. The dashed lines connecting our observations for the surface-water oxygenation reflect our belief that surface-water oxygenation was a continuous feature through the last half of the Neoproterozoic.

conditions were more common, and that episodes of deep-water oxygenation preceded the Gaskiers or even earlier glaciations. Future work should resolve this.

In the modern world, and through much of the Phanerozoic Eon (*19*), marine anoxia produces sulfidic conditions. Why was this not generally true in the later Neoproterozoic? The persistence of Fe in anoxic deep waters requires that the molar flux of FeHR to the deep ocean be greater than half the flux of sulfide, the ratio needed to give excess Fe after the formation of FeS_2 (*3*). Therefore, to explain Neoproterozoic ferruginous deep-water chemistry, we must appeal to factors that either limited S input to the ocean or increased the input of Fe. Indeed, both may have been in play. Previous modeling has suggested that the surface inventory of S may have decreased in size through the Mesoproterozoic and into the Neoproterozoic because of the subduction of sedimentary sulfides deposited beneath sulfidic ocean waters (*32*). This would have made less S available for weathering and reduced the flux of sulfate to the ocean. Furthermore, Neoproterozoic sulfate concentrations were probably much less than today (*32*, *33*). Reduced sulfate levels change the redox balance during mid–ocean ridge hydrothermal circulation, resulting in an increased flux of Fe from hydrothermal fluids to the oceans (*34*). We propose that these processes, either singly or combined, produced the chemistry of later Neoproterozoic oceans.

References and Notes

1. H. D. Holland, *The Chemical Evolution of the Atmosphere and Oceans* (Princeton Univ. Press, Princeton, NJ, 1982).
2. D. E. Canfield, K. S. Habicht, B. Thamdrup, *Science* **288**, 658 (2000).
3. D. E. Canfield, *Nature* **396**, 450 (1998).
4. C. Scott *et al.*, *Nature* **452**, 456 (2008).
5. Y. Shen, A. H. Knoll, M. R. Walter, *Nature* **423**, 632 (2003).
6. S. W. Poulton, P. W. Fralick, D. E. Canfield, *Nature* **431**, 173 (2004).
7. H. D. Holland, *Philos. Trans. R. Soc. London Ser. B* **361**, 903 (2006).
8. A. H. Knoll, S. B. Carrol, *Science* **284**, 2129 (1999).
9. P. F. Hoffman, *S. Afr. J. Geol.* **108**, 557 (2005).
10. J. L. Kirschvink, *Am. Assoc. Pet. Geol. Bull.* **75**, 610 (1991).
11. P. F. Hoffman, A. J. Kaufman, G. P. Halverson, D. P. Schrag, *Science* **281**, 1342 (1998).
12. D. E. Canfield, S. W. Poulton, G. M. Narbonne, *Science* **315**, 92 (2007).
13. S. W. Poulton, D. E. Canfield, *Chem. Geol.* **214**, 209 (2005).
14. R. Raiswell, D. E. Canfield, *Am. J. Sci.* **298**, 219 (1998).
15. Materials and methods are available as supporting material on *Science* Online.
16. We have tried to avoid weathering by collecting in the field the freshest material possible, and furthermore, we have removed any further evidence of weathering when preparing samples for crushing, powdering, and eventual chemical extraction. Still, oxidative weathering is possible in some cases. The main influence of weathering will be to oxidize reduced-Fe phases such as FeS_2 and Fe carbonates to Fe oxides. In this way, the total reactive Fe content of the sample would be little affected, although the distribution of phases might be. For this reason, some of our FeS_2 and Fe carbonate contents may be underestimated. This is probably the worst for our Sheepbed samples, although all of these still retain FeS_2, sometimes in appreciable amounts (*15*). Nonetheless, even if we underestimate the FeS_2 and Fe carbonate contents of some samples because of weathering, our evaluation of the nature of ocean chemistry, and particularly the dominance of ferruginous conditions, is generally not affected. This is because although some Fe carbonate may have been lost, the Fe carbonate contents of most samples are high enough to preclude deposition in a sulfidic water column—even making the extreme (and probably incorrect) assumption that all Fe oxides represent oxidized FeS_2.
17. D. Z. Oehler, J. H. Oehler, A. J. Stewart, *Science* **205**, 388 (1979).
18. J. W. Green, A. H. Knoll, K. Swett, *Geol. Mag.* **126**, 567 (1989).
19. S. W. Poulton, R. Raiswell, *Am. J. Sci.* **302**, 774 (2002).
20. K. K. Turekian, K. H. Wedepohl, *Geol. Soc. Am. Bull.* **72**, 175 (1961).
21. T. W. Lyons, S. Severmann, *Geochim. Cosmochim. Acta* **70**, 5698 (2006).
22. G. M. Ross, J. D. Bloch, H. R. Krouse, *Precambrian Res.* **73**, 71 (1995).
23. D. A. Fike, J. P. Grotzinger, L. M. Pratt, R. E. Summons, *Nature* **444**, 744 (2006).
24. K. A. McFadden *et al.*, *Proc. Natl. Acad. Sci. U.S.A.* **105**, 3197 (2008).
25. Y. Shen, T. Zhang, P. F. Hoffman, *Proc. Natl. Acad. Sci. U.S.A.* **105**, 7376 (2008).
26. C. M. Dehler *et al.*, *Sediment. Geol.* **141**, 465 (2001).
27. K. E. Karlstrom *et al.*, *Geology* **28**, 619 (2000).
28. T. Goldberg, H. Strauss, Q. Guo, C. Liu, *Palaeogeogr. Palaeoclimatol. Palaeoecol.* **254**, 175 (2007).
29. B. Lehmann *et al.*, *Geology* **35**, 403 (2007).
30. H. Kimura, Y. Watanabe, *Geology* **29**, 995 (2001).
31. S. Schroder, J. P. Grotzinger, *J. Geol. Soc. London* **164**, 175 (2007).
32. D. E. Canfield, *Am. J. Sci.* **304**, 839 (2004).
33. L. C. Kah, T. W. Lyons, T. D. Frank, *Nature* **431**, 834 (2004).
34. L. R. Kump, W. E. Seyfried Jr., *Earth Planet. Sci. Lett.* **235**, 654 (2005).

35. For financial support, we thank Danmarks Grundforskningsfond, the Natural Environment Research Council (research fellowship to S.W.P.), NSF (Division of Earth Sciences grant 0420592 to A.H.K.), and the Natural Sciences and Engineering Research Council of Canada Discovery Grant, Northwest Territories Scientist's License. We acknowledge the help of N. P. James and T. K. Kyser; the insightful comments of D. Johnston; and the expert technical assistance of L. Salling, M. Andersen, and E. Hammarlund.

Supporting Online Material

www.sciencemag.org/cgi/content/full/1154499/DC1
Materials and Methods
Figs. S1 and S2
Table S1
References

21 December 2007; accepted 2 July 2008
Published online 17 July 2008;
10.1126/science.1154499
Include this information when citing this paper.

Plant Immunity Requires Conformational Charges of NPR1 via S-Nitrosylation and Thioredoxins

Yasuomi Tada,[1] Steven H. Spoel,[1] Karolina Pajerowska-Mukhtar,[1] Zhonglin Mou,[1]* Junqi Song,[1] Chun Wang,[2] Jianru Zuo,[2] Xinnian Dong[1]†

Changes in redox status have been observed during immune responses in different organisms, but the associated signaling mechanisms are poorly understood. In plants, these redox changes regulate the conformation of NPR1, a master regulator of salicylic acid (SA)–mediated defense genes. NPR1 is sequestered in the cytoplasm as an oligomer through intermolecular disulfide bonds. We report that S-nitrosylation of NPR1 by *S*-nitrosoglutathione (GSNO) at cysteine-156 facilitates its oligomerization, which maintains protein homeostasis upon SA induction. Conversely, the SA-induced NPR1 oligomer-to-monomer reaction is catalyzed by thioredoxins (TRXs). Mutations in both NPR1 cysteine-156 and TRX compromised NPR1-mediated disease resistance. Thus, the regulation of NPR1 is through the opposing action of GSNO and TRX. These findings suggest a link between pathogen-triggered redox changes and gene regulation in plant immunity.

Innate immune responses are evolutionarily conserved among plants and animals (*1*, *2*) and are often associated with changes in cellular oxidative and reductive states. In plants, these redox changes are sensed by the NPR1 protein, a master regulator of defense gene expression (*3*). In unchallenged plants, NPR1 resides in the cytoplasm as an oligomer maintained through redox-sensitive intermolecular disulfide bonds. Upon pathogen challenge, the plant defense signaling molecule salicylic acid (SA) increases and changes the cellular redox state, leading to reduction of the disulfide bonds in NPR1. Reduction of the NPR1 oligomer releases monomer that translocates to the nucleus where it activates the expression of a battery of *pathogenesis-related* (*PR*) genes (*4*). Mutations at residues Cys^{82} and Cys^{216} in NPR1 result in increased monomer accumulation, constitutive nuclear localization, and NPR1-mediated gene expression in the absence of pathogen challenge (*3*). On the basis of these results, it has been proposed that conformational changes in NPR1 (that is, oligomer-monomer exchange) regulate its nuclear translocation and activity (*3*).

Oligomerization of proteins through intermolecular disulfide bonds is unusual under reductive cytosolic conditions (*5*). However, treatment with SA not only induced NPR1 monomer release but also facilitated oligomerization in wild-type plants (fig. S1A). Similar results were obtained with biologically active NPR1 fused with green fluorescent protein (NPR1-GFP) (*4*) or with tandem affinity purification tag (NPR1-TAP) (fig.